

**Supporting Information****Ionic Matrix for Enhanced MALDI Imaging Mass Spectrometry for Identification of  
Phospholipids in Mouse Liver and Cerebellum Tissue Sections**

**Kamlesh Shrivastava, Takahiro Hayasaka, Naoko Goto-Inoue, Yuki Sugiura, Nobuhiro Zaima,  
Mitsutoshi Setou\***

Department of Molecular Anatomy, Molecular Imaging Frontier Research Center, Hamamatsu  
University School of Medicine, 1-20-1 Handayama, Higashi-ku, Hamamatsu, Shizuoka 431-3192,  
Japan

\*Corresponding author. Tel/Fax: +81-53-435-2292; E-mail: setou@hama-med.ac.jp

**Solution Preparations.** Each mixture solution of PC, SM, PS, and PI (3 mg/mL, Avanti Polar Lipids) was diluted to working standards with methanol and aliquots of 40 pmol/ $\mu$ L of lipid mixtures were used for MALDI-IMS analysis in order to demonstrate the homogeneity, reproducibility, and signal enhancement of phospholipids. CHCA, DHB, CHCAB and DHBB matrix solutions were prepared at the concentration of 20 mg/mL in 75% methanol/0.1% TFA for the analysis of standard phospholipid mixtures and that of 40 mg/mL in 75% methanol/0.1% TFA for deposition onto the mouse liver and cerebellum tissue sections prior to MALDI-IMS analysis, respectively. Similarly, AA, DHAP and PNA were prepared at the concentration of 20 mg/mL, 30 mg/mL and 30 mg/mL, respectively in 75% methanol/0.1% TFA for the application of matrix onto the mouse liver tissue sections, respectively. The concentration of matrix solution used in this study was optimized for the identification of phospholipids in tissue sections.

**Effect of Solvents in the Matrix Solution for Identification of Phospholipids in Mouse Liver Tissue Sections.** The percentage of organic solvent in the matrix solution must be carefully considered before matrix application because these parameters affect the crystal formation with analyte molecules on the surface of tissue sections for identification of biomolecules and ion images. The amount and type of solvent applied on the tissue should allow efficient extraction of different types of biomolecules from the surface of tissue sections.<sup>1,2</sup> Thus, we prepared DHB and CHCAB at different percentages (20%, 40%, 60% and 75%) of organic solvents (acetonitrile or methanol) with 0.1% TFA. We avoided the use of 100% organic solvent because in a previous study (Sugiura *et al.*)<sup>3</sup> it was reported that the use of a higher percentage (90-100%) was not advisable because the organic solvent evaporated before reaching the target plate. Figures S1A to S1H show the MALDI-IMS spectra of phospholipids in mouse live tissue sections by using CHCAB as a matrix with acetonitrile and methanol. The application of 75% methanol to the matrix

solution gave a good signal intensity and number of phospholipids from the surface of the tissue section. Methanol has been reported to be a good solvent for the preparation of matrix solution for detection of lipid molecules from tissue sections. Therefore, 75% methanol (containing 0.1% TFA) was selected as a solvent for matrix application on the surface of tissue sections.

The analyte spreading is an important issue in IMS studies if the tissue section is too wet after the matrix application. Thus, care must be taken during the deposition of IM on the surface of tissue sections in order to prevent the analyte spreading, and the best way to maintain the distance between the sprayer and tissue section. In the present study, the diffusion of analyte can't be differentiated because the analyses were performed at the resolution of 50  $\mu\text{m}$  (scan pitch) that was very low to confirm it. However, the images of lipids obtained in mouse cerebellum tissue section shown in Figures 3B and 3C showed the clear ion images at the different edges of the tissue section.

**Identification of Phospholipids by MALDI-IMS in Negative Ion Mode.** A wide variation in the signal intensity of ion images for PI and PS species were obtained when DHB and CHCA were used as matrixes, as shown in Figures S2A and S2B, respectively. This might have been due to the nonhomogeneity in the crystal formation with analytes that caused improper desorption and ionization of phospholipids present on the surface of the sample. Conversely, better ion images were observed when DHBB IM was used for the identification of phospholipids in negative ion mode with little coarseness in the intensity, as can be seen in Figure S2C. However, ion images of almost equal signal intensity were acquired when CHCAB IM was used for the detection of PI and PS in MALDI-IMS analysis in negative ion mode (Figure S2D). Thus, the use of CHCAB IM was found to have more potential than the use of any other matrixes for the identification of PI and PS by MALDI-IMS analysis. The enhancement of signal intensity was also investigated in negative ion mode by selecting 30 ROI points of the given images of the respective species of PI and PS from

the mass spectrum. Improvements of 6-18 fold in the signal intensity were obtained when CHCAB IM was used as a matrix for desorption and ionization of PI and PS in MALDI-IMS as compared to other matrixes. Therefore, CHCAB IM could also be used as a better matrix for imaging of acidic phospholipids by MALDI-IMS in negative ion mode.

**Operating Conditions for MALDI MS/MS Analysis of Phospholipids.** MALDI-MS/MS analyses of lipids found in mouse liver and cerebellum tissue sections were performed using a quadrupole-TOF tandem mass spectrometer with an orthogonal MALDI source attached (QSTAR Elite: Applied Biosystems/MDS Sciex, Thornhill, Ontario, Canada). The purpose of MS/MS analyses of phospholipids in mouse tissue sections was to confirm the type of species of lipids present in the tissue samples. The collisional activation of selected ions was carried out by using relative collision energy from 45 to 70 eV with argon as a collision gas. Before the MS/MS analysis, the instrument was calibrated with bradykinin and angiotensin II at  $m/z$  757.39  $[M+H]^+$  and 1046.54  $[M+H]^+$  in positive ion mode and 755.34  $[M-H]^-$  and 1044.54  $[M-H]^-$  in negative ion mode. A 355-nm wavelength laser beam was used for the irradiation of samples with a repetition rate of 1000 Hz, and the laser energy was varied to obtain a good MS/MS spectrum of phospholipids. A Human Metabolome database search (<http://www.hmdb.ca/labm/jsp/mlims/MSDbParent.jsp>) provided the information regarding the number of carbon and unsaturated bonds present in the phospholipids from mouse tissue samples.

**MS/MS Analysis of Phospholipids in Mouse Liver Tissue Sections.** Analysis of phospholipids in mouse liver tissue sections by MALDI-IMS allowed the assignment of lipid molecules in tissue samples. Thus, MS/MS analysis of molecules is necessary in order to characterize the detailed structure and composition of target molecules in tissue sections. For this purpose, the surfaces of liver tissue sections were sprayed with 1 mL of respective matrix solution and then analyzed by

MS/MS in the positive ion mode. Figures S4A and S4B represent the product-ion spectra of protonated  $[M+H]^+$  and sodiated  $[M+Na]^+$  species of PC in liver tissue sections. Figure S4A shows the results of the MS/MS analysis of the biomolecules observed at  $m/z$  758.53  $[M+H]^+$  in mouse liver tissue sections. The peaks observed at  $m/z$  502.42  $[M-16:0+H]^+$  and 478.45  $[M-18:2+H]^+$  corresponded to the loss of fatty acids from molecular ions. The number of carbon and fatty acid unsaturations was also confirmed by a Human Metabolome Database Search. The major prominent peak detected at  $m/z$  184.05  $[(CH_3)_3 N(CH_2)_2 PO_4 H+H]^+$  represented the phosphatidylcholine, the head group of PC or SM, which confirmed the existence of protonated ions of phospholipids in positive ion mode.<sup>3,4</sup> The protonated PC molecules appeared at even  $m/z$  values, whereas the protonated molecules of SM appeared at odd  $m/z$  values due to the presence of an additional nitrogen atom in SM.<sup>5</sup> Thus, based on the fragmentation of molecules in Figure S4A, the signal at  $m/z$  758.53 was assigned to be  $[PC(16:0/18:2)+H]^+$ . Subsequently, the same types of product-ion spectra for protonated molecules of PC were obtained with mass peaks at  $m/z$  782.54  $[PC(16:0/20:4)+H]^+$ , 786.56  $[PC(18:1/18:1)+H]^+$ , 806.54  $[PC(16:0/22:6)+H]^+$ , 810.57  $[PC(18:0/20:4)+H]^+$  and 834.56  $[PC(18:0/22:6)+H]^+$ , as shown in Table S1. Figure S4B displays the product-ion spectrum for sodiated molecular ions at  $m/z$  780.51  $[M+Na]^+$  in liver tissue sections, where the neutral loss of 59 and 183 Da, and formation of sodium adducts at  $m/z$  721.47  $[M-59+Na]^+$  and 597.48  $[M-183+Na]^+$  with molecular ions were found to be common. The peak generated at  $m/z$  575.49  $[M-183+H]^+$  showed a mass difference of 21.99 units (loss of sodium ion) from the peak at  $m/z$  597.48, thereby verifying the presence of sodium ions in the tissue section. In addition, the peaks identified at  $m/z$  465.24  $[M-59-16:0+Na]^+$  and 441.23  $[M-59-18:2+Na]^+$  illustrated the loss of the respective fatty acids from molecular ions. We also observed peaks at  $m/z$  184.06 and 146.97, which were associated with protonated ions of the phosphatidylcholine head group  $[(CH_3)_3$

$N(CH_2)_2 PO_4H+H]^+$  and sodiated cyclophosphane ring  $[(CH_2)_2PO_4+Na]^+$ . Hence, the biomolecules found in liver tissue sections was assigned as  $[PC(16:0)/18:2)+Na]^+$ . In the same way, a fragmentation pattern of sodium and potassium adducted PC species was observed in the mass spectrum at  $m/z$  832.55  $[PC(18:0/20:4)+Na]^+$ , 772.48  $[PC(16:0/16:0)+K]^+$ , 796.50  $[PC(16:0/18:2)+K]^+$ , 798.53  $[PC(16:0/18:1)+K]^+$ , 820.51  $[PC(16:0/20:4)+K]^+$ , 822.51  $[PC(18:1/18:2)+K]^+$ , 824.52  $[PC(18:0/18:2)+K]^+$ , 844.52  $[PC(16:0/22:6)+K]^+$ , 848.52  $[PC(18:0/20:4)+K]^+$  and 872.52  $[PC(18:0/22:6)+K]^+$  listed in Table S1. MS/MS analysis of the protonated, sodiated and potassiated species of PC was in agreement with our previous studies in the positive ion mode in mouse tissue samples.<sup>3,6</sup>

We also observed the presence of PE and PS phospholipid species in liver tissue sections to which PC had been added by the proposed method of MALDI-IMS analyses in the positive ion mode. Figure S4C shows the product-ion spectrum of PE with sodiated molecular ions at  $m/z$  738.48  $[M+Na]^+$ . The peaks identified at  $m/z$  695.50  $[M-43+Na]^+$  and 597.48  $[M-141+Na]^+$  represent the neutral loss of aziridine  $(CH_2)_2NH$  and phosphoethanolamine  $(HPO_4)(CH_2)_2NH_3$ , respectively. The losses of 43 and 141 Da from molecular ions were indicative of the head group and characteristics of PE phospholipid species in the liver tissue sections.<sup>7</sup> The peak detected at  $m/z$  575.51  $[M-141+H]^+$  showed the loss of sodium ions (21.97 unit) from the mass peak at  $m/z$  597.48. The spectrum also contained fragmented ions at  $m/z$  415.20  $[M-43-18:2+Na]^+$ , which raised from neutral loss of fatty acids from parent ions. In addition, the molecule observed at  $m/z$  738.48 was investigated by a Human Metabolome Database Search to confirm the composition of fatty acids present in PE. Thus in the present study, the molecule was assigned to be  $[PE(16:0/18:2)+Na]^+$ . Next, the fragmentation pattern of PS at  $m/z$  812.51  $[M+Na]$  from liver tissue sections was investigated, as shown in Figure S4D. The neutral loss of 87 Da  $(C_3H_5O_2N)$  at  $m/z$  725.49  $[M-$

$87+\text{Na}]^+$  and 185 Da ( $\text{NH}_3\text{CH}(\text{CO}_2\text{H})\text{CH}_2\text{PO}_4\text{H}$ ) from molecular ions at  $m/z$  627.53  $[\text{M}-185+\text{Na}]$  showed the presence of a head group of PS molecules. The loss of fatty acid at  $m/z$  441.23  $[\text{M}-87-18:0+\text{Na}]^+$  and formation of sodium adduct with a polar head group  $[(\text{NH}_3\text{CH}(\text{CO}_2\text{H})\text{CH}_2\text{PO}_4\text{H})+\text{Na}]^+$  at  $m/z$  207.99 verified the existence of PE in mouse liver tissue sections. The Human Metabolome Database search was used to investigate the constituents of fatty acids for the mass peak observed at  $m/z$  812.51, which was assigned to be  $\text{PS}(18:0/20:4)+\text{Na}]^+$ . Hence, the presence of phospholipids obtained in mouse liver tissue sections [listed in Tables S1 and S2] was verified by MS/MS analyses. The use of CHCAB IM in MALDI-IMS analysis of mouse liver tissue sections helped in identifying a wider range of phospholipids compared to DHB, DHBB, CHCA, AA, PNA and DHAP matrixes.

**MS/MS Analysis of Phospholipids in the Mouse Cerebellum Tissue Sections.** MS/MS analysis of mouse cerebellum tissue sections was performed in order to verify the ion images of phospholipid species detected in Figures 3B and 3C and Table 1. The lipids found were protonated, sodiated and potassiated species of PC, SM, PS and GalCer in cerebellum tissue sections. The fragmentation pattern of phospholipids (PC, SM, and PS) was similar to the product-ion spectra of lipids found during the MS/MS analyses of liver tissue sections. Additionally, we observed an additional lipid molecule of GalCer in the mouse cerebellum by using CHCAB IM in MALDI-IMS analysis. Thus, MS/MS analyses and a Human Metabolome Database Search confirmed the species and composition of fatty acids present in molecule of GalCer. The neutral loss of 18 Da ( $\text{H}_2\text{O}$ ), 162 Da ( $\text{C}_6\text{H}_{10}\text{O}_5$ ) and 180 Da ( $\text{C}_6\text{H}_{12}\text{O}_6$ ) from molecular ions revealed that the molecules corresponded to GalCer (data not shown). A similar fragmentation pattern of GalCer has also been reported in the literature.<sup>8</sup>

## References

- (1) Sugiura, Y.; Setou, M. *Rapid Commun. Mass Spectrom.* **2009**, 23, 3269–3278.
- (2) Kaletas, B. K.; van der Wiel, I. M.; Stauber, J.; Guzel, C.; Kros J. M.; Luider, T. M.; Heeren R. M. A. *Proteomics* **2009**, 9, 2622–2633.
- (3) Hayasaka, T.; Goto-Inoue, N.; Zaima, N.; Kimura, Y.; Setou, M. *Lipids* **2009**, 44, 837–848.
- (4) Jackson, S. N.; Wang, H. Y. J.; Woods, A. S. *Anal. Chem.* **2005**, 77, 4523–4527.
- (5) Brugger, B.; Erben, G.; Sandoff, R.; Wieland, F. T.; Lehmann, W. D. *Proc. Natl. Acad. Sci. USA*, **1997**, 94, 2339–2344.
- (6) Sugiura, Y.; Konishi, Y.; Zaima, N.; Kajihara, S.; Nakanishi, H.; Taguchi R.; Setou, M. *J. Lipid. Res.* **2009**, 50, 1776–1788.
- (7) Hsu, F. F.; Turk, J. J. *Mass Spectrom.* **2000**, 35, 596–606.
- (8) Jackson, S. N.; Ugarov, M. Egan, T.; Post, J. D.; Langlais, D.; Schultz, A.; Woods A. S. *J. Mass Spectrom.* **2007**, 42: 1093–1098.



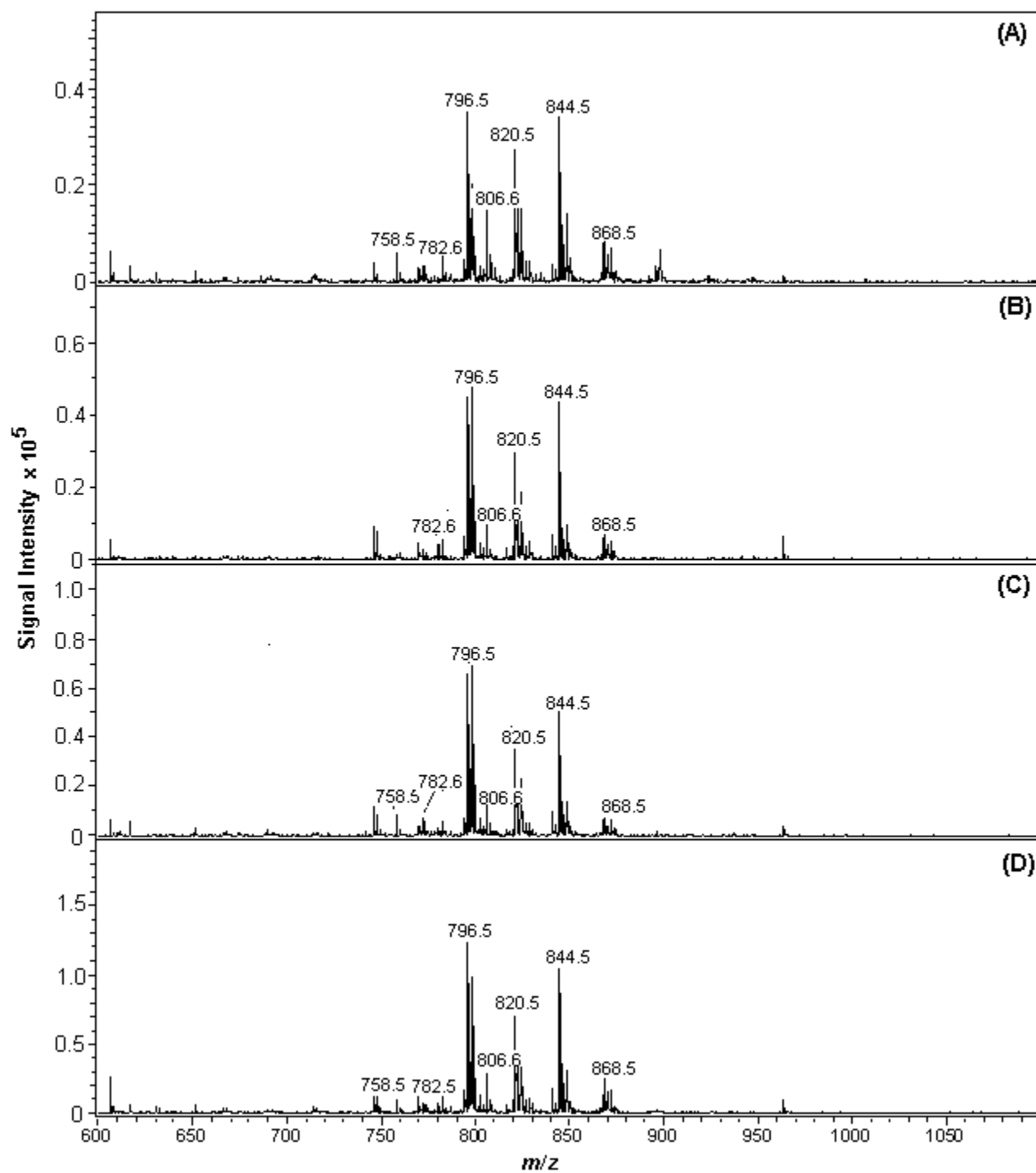


**Figure S1.** Effect of different percentage of acetonitrile (A) 20%, (B) 40%, (C) 60%, and (D) 75 % in the matrix solution (CHCAB) for the identification of phospholipids in mouse liver tissue sections.

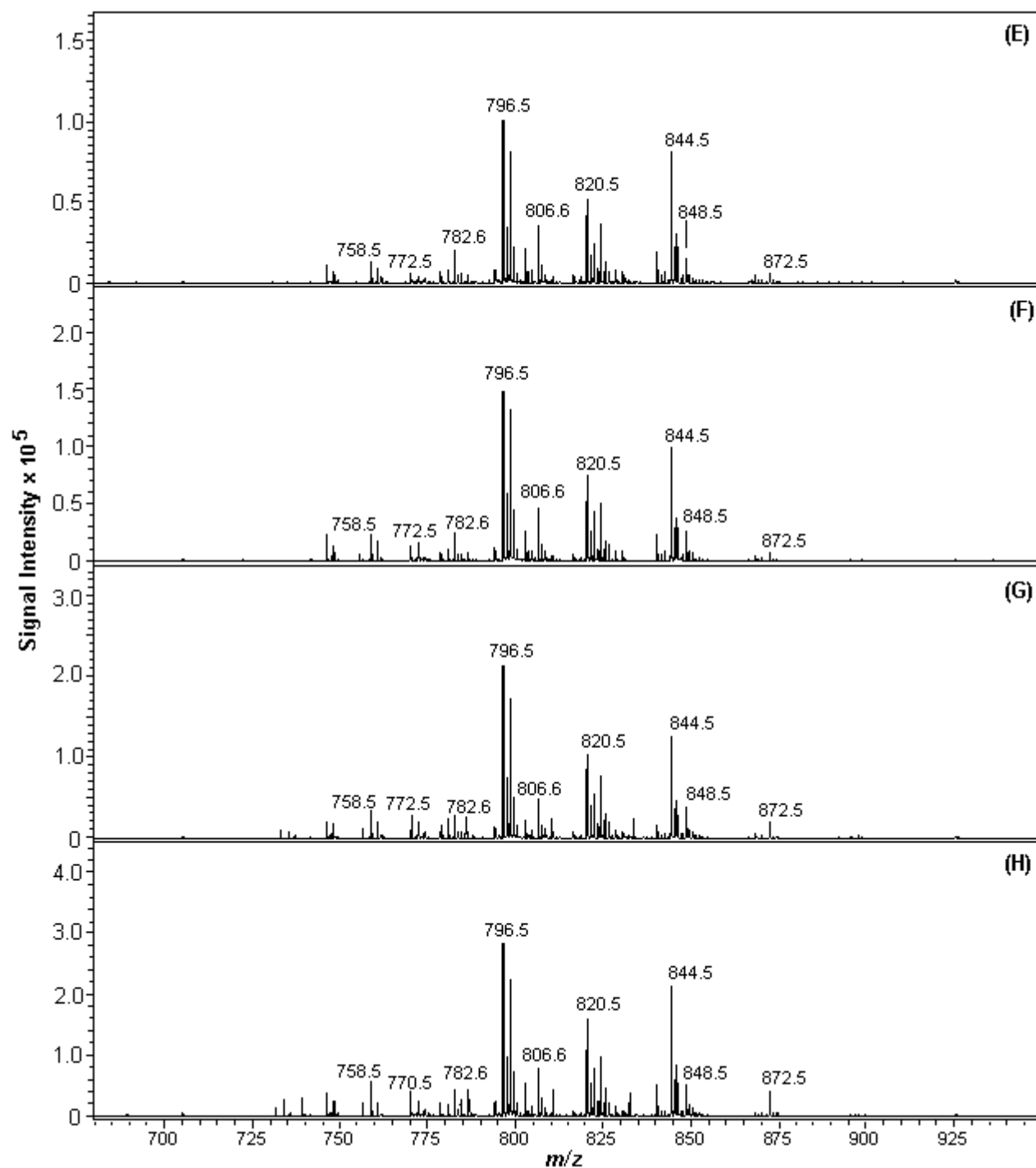


**Figure S1.** Effect of different percentage of methanol (E) 20%, (F) 40%, (G) 60%, and (H) 75 % in the matrix solution (CHCAB) for the identification of phospholipids in mouse liver tissue sections.

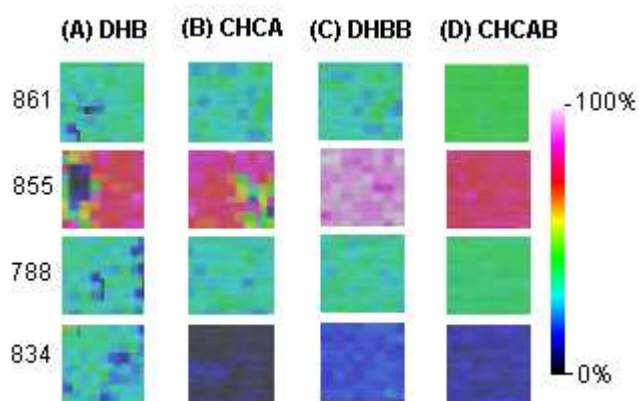


**Figure S2.** Ion image of phospholipids of PI and PS reconstructed from MALDI-IMS analyses at  $m/z$  861 [PI(18:0/18:2)-H]<sup>-</sup>, 855 [PI(18:0/20:4)-H]<sup>-</sup>, 788 [PS(18:0/18:1)-H]<sup>-</sup> and 834 [PS(18:0/22:6)-H]<sup>-</sup> by using (A) DHB: wide variation in signal intensity; (B) CHCA: variation in signal intensity; (C) DHBB: less variation of signal intensity than CHCA and DHB matrixes; and (D) CHCAB: almost same signal intensity observed throughout the ion image.

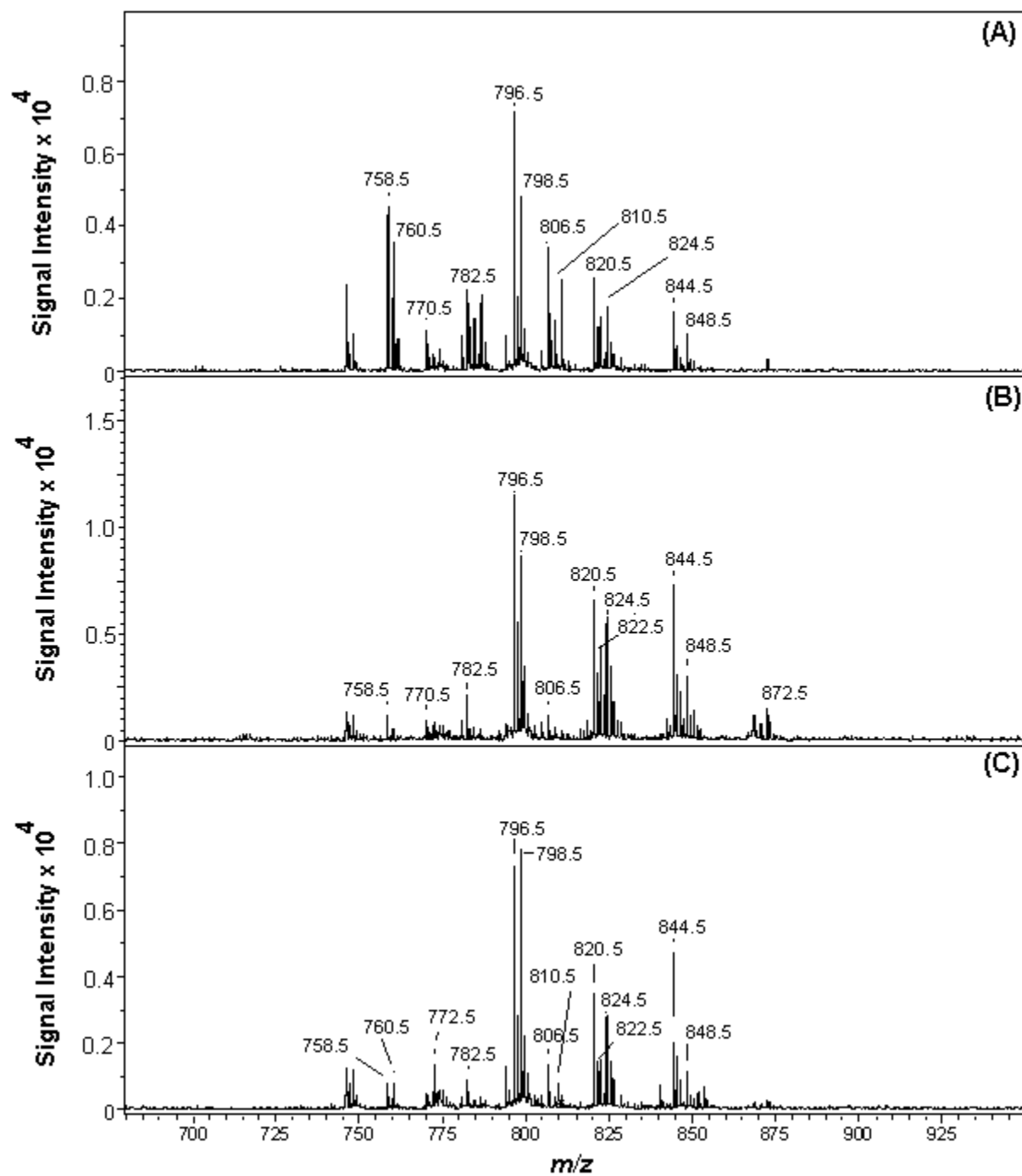


**Figure S3:** MALDI-IMS spectra of phospholipids of mouse liver tissue sections obtained with (A) AA, (B) PNA, and (C) DHAP matrixes. The identified molecular species of phospholipids obtained by different matrixes are summarized in Table S2.

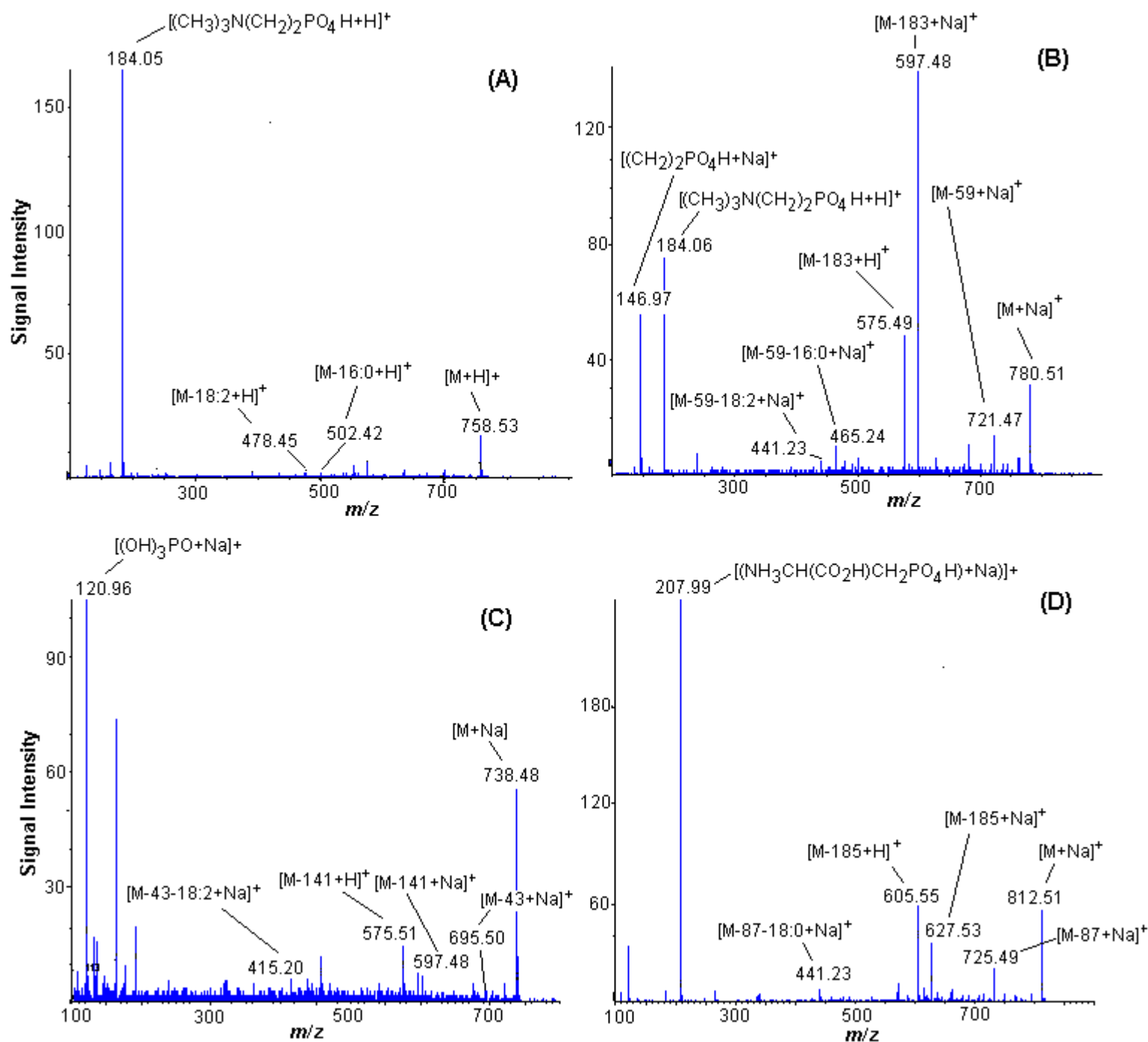


**Figure S4.** Product-ion spectra of (A) protonated molecular ions  $[M+H]^+$  at  $m/z$  758.53 [PC(16:0/18:2)+H] $^+$ ; (B) Sodiated molecular ions  $[M+Na]^+$  at  $m/z$  780.51 [PC(16:0/18:2)+Na] $^+$ ; (C) Sodiated molecular ions  $[M+Na]^+$  at  $m/z$  738.48 [PE(16:0/18:2)+Na] $^+$ ; and (D) sodiated molecular ions at  $m/z$  812.51 [PS(18:0/20:4)+Na] $^+$  in mouse liver tissue sections.

**Table S1.** Species of Phospholipids identified in liver tissue sections by using DHB, DHBB, CHCA and CHCAB IM as a matrix in positive ion mode (Confirmed by MS/MS analyses)

Matrixes	Experimental mass ( $m/z$ )	Theoretical mass ( $m/z$ )	Molecular species of phospholipids
DHB	758.53	758.57	PC(16:0/18:2)+H
	772.48	772.53	PC(16:0/16:0)+K
	782.54	782.57	PC(16:0/20:4)+H
	786.56	786.60	PC(18:1/18:1)+H
	796.50	796.53	PC(16:0/18:2)+K
	798.53	798.54	PC(16:0/18:1)+K
	806.54	806.57	PC(16:0/22:6)+H
	810.57	810.60	PC(18:0/20:4)+H
	822.51	822.54	PC(18:1/18:2)+K
	824.52	824.56	PC(18:0/18:2)+K
	834.56	834.60	PC(18:0/22:6)+H
	844.51	844.53	PC(16:0/22:6)+K
	848.52	848.56	PC(18:0/20:4)+K
	872.52	872.56	PC(18:0/22:6)+K
DHBB	758.52	758.57	PC(16:0/18:2)+H
	770.49	770.51	PC(16:0/16:1)+K
	772.51	772.53	PC(16:0/16:0)+K
	782.55	782.57	PC(16:0/20:4)+H
	786.57	786.60	PC(18:1/18:1)+H
	796.49	796.53	PC(16:0/18:2)+K
	798.52	798.54	PC(16:0/18:1)+K
	806.54	806.57	PC(16:0/22:6)+H
	810.55	810.60	PC(18:0/20:4)+H
	822.50	822.54	PC(18:1/18:2)+K
	824.52	824.56	PC(18:0/18:2)+K
	834.54	834.60	PC(18:0/22:6)+H
	844.50	844.53	PC(16:0/22:6)+K
	848.52	848.56	PC(18:0/20:4)+K
	872.53	872.56	PC(18:0/22:6)+K
CHCA	758.54	758.57	PC(16:0/18:2)+H
	782.54	782.57	PC(16:0/20:4)+H
	796.50	796.53	PC(16:0/18:2)+K
	806.54	806.57	PC(16:0/22:6)+H
	810.56	810.60	PC(18:0/20:4)+H
	820.51	820.53	PC(16:0/20:4)+K
	824.50	824.56	PC(18:0/18:2)+K

CHCAB	844.52	844.53	PC(16:0/22:6)+K
	738.48	738.50	PE(16:0/18:2)+Na
	756.51	756.55	PC(16:0/18:3)+H
	758.55	758.57	PC(16:0/18:2)+H
	770.50	770.51	PC(16:0/16:1)+K
	772.51	772.53	PC(16:0/16:0)+K
	780.51	780.55	PC(16:0/18:2)+Na
	782.56	782.57	PC(16:0/20:4)+H
	786.58	786.60	PC(18:1/18:1)+H
	788.58	788.62	PC(18:1/18:0)+H
	796.51	796.53	PC(16:0/18:2)+K
	798.53	798.54	PC(16:0/18:1)+K
	806.53	806.57	PC(16:0/22:6)+H
	810.58	810.60	PC(18:0/20:4)+H
	812.51	812.54	PS(18:0/20:4)+Na
	820.51	820.53	PC(16:0/20:4)+K
	822.50	822.54	PC(18:1/18:2)+K
	824.53	824.56	PC(18:0/18:2)+K
	832.55	832.58	PC(18:0/20:4)+Na
	834.56	834.60	PC(18:0/22:6)+H
	844.50	844.53	PC(16:0/22:6)+K
	848.53	848.56	PC(18:0/20:4)+K
	852.49	852.52	PS(18:0/20:3)+K
	872.52	872.56	PC(18:0/22:6)+K

---

**Table S2.** Species of Phospholipids identified in liver tissue sections by using AA, PNA and DHAP as a matrix in positive ion mode (Confirmed by MS/MS analyses)

Matrixes	Experimental mass ( $m/z$ )	Theoretical mass ( $m/z$ )	Molecular species of phospholipids
AA	758.51	758.57	PC(16:0/18:2)+H
	760.53	760.59	PC(16:0/18:1)+H
	770.50	770.51	PC(16:0/16:1)+K
	780.50	780.55	PC(16:0/18:2)+Na
	782.53	782.57	PC(16:0/20:4)+H
	786.54	786.60	PC(18:1/18:1)+H
	796.49	796.53	PC(16:0/18:2)+K
	798.51	798.54	PC(16:0/18:1)+K
	806.51	806.57	PC(16:0/22:6)+H
	810.54	810.60	PC(18:0/20:4)+H
	820.52	820.53	PC(16:0/20:4)+K
	822.49	822.54	PC(18:1/18:2)+K
	824.52	824.56	PC(18:0/18:2)+K
	844.49	844.53	PC(16:0/22:6)+K
	848.52	848.56	PC(18:0/20:4)+K
PNA	758.51	758.57	PC(16:0/18:2)+H
	770.51	770.51	PC(16:0/16:1)+K
	782.52	782.57	PC(16:0/20:4)+H
	796.50	796.53	PC(16:0/18:2)+K
	798.49	798.54	PC(16:0/18:1)+K
	806.52	806.57	PC(16:0/22:6)+H
	820.50	820.53	PC(16:0/20:4)+K
	822.53	822.54	PC(18:1/18:2)+K
	824.51	824.56	PC(18:0/18:2)+K
	844.49	844.53	PC(16:0/22:6)+K
DHAP	848.50	848.56	PC(18:0/20:4)+K
	872.53	872.56	PC(18:0/22:6)+K
	758.52	758.57	PC(16:0/18:2)+H
	760.54	760.59	PC(16:0/18:1)+H
	772.49	772.53	PC(16:0/16:0)+K
	782.52	782.57	PC(16:0/20:4)+H
	796.50	796.53	PC(16:0/18:2)+K
	798.51	798.54	PC(16:0/18:1)+K
	806.54	806.57	PC(16:0/22:6)+H
	810.54	810.60	PC(18:0/20:4)+H
	820.49	820.53	PC(16:0/20:4)+K
	822.53	822.54	PC(18:1/18:2)+K
	824.50	824.56	PC(18:0/18:2)+K
	844.48	844.53	PC(16:0/22:6)+K
	848.52	848.56	PC(18:0/20:4)+K



**Table S3.** List of peptide sequence for tryptic digested cytochrome c observed in MALDI-MS spectra by using CHCA and CHCAB as a matrix

Observed ( <i>m/z</i> ) by CHCA	Observed ( <i>m/z</i> ) by CHCAB	Peptide sequence
634.3	634.3	IFVQK
678.3	678.3	YIPGTK
-	762.5	KIFVQK
779.5	779.5	MIFAGIK
-	795.4	MIFAGIK (Oxidation, M)
817.4	817.4	CAQCHTVEK
907.5	907.5	MIFAGIKK
-	923.5	MIFAGIKK (Oxidation, M)
1168.5	1168.5	TGPNLHGLFGR
1296.6	1296.6	TGPNLHGLFGRK
1434.6	1434.6	GEREDLIAYLKK
1456.6	1456.6	TGQAPGFSYTDANK
1478.5	1478.5	TEREDLIAYLKK
1561.6	1561.6	HKTGPNLHGLFGRK
-	1606.6	KTEREDLIAYLKK
-	1623.6	EETLMEYLENPKK
1633.4	1633.4	IFVQKCAQCHTVEK
-	1826.7	KTGQAPGFSYTDANKN